The Journal of Chemical Physics

Time resolved detection of the S(^{1}D) product of the UV induced dissociation of CS_2

Cite as: J. Chem. Phys. **154**, 034302 (2021); https://doi.org/10.1063/5.0035045
Submitted: 26 October 2020 • Accepted: 26 December 2020 • Published Online: 15 January 2021

Emily M. Warne, Adam D. Smith, Daniel A. Horke, et al.

The Journal of Chemical Physics ARTICLE scitation.org/journal/jcp

Time resolved detection of the S(^{1}D) product of the UV induced dissociation of CS_2

Cite as: J. Chem. Phys. 154, 034302 (2021); doi: 10.1063/5.0035045
Submitted: 26 October 2020 • Accepted: 26 December 2020 •
Published Online: 15 January 2021

Emily M. Warne,[1] Adam D. Smith,[1] Daniel A. Horke,[2,3,4] Emma Springate,[5] Alfred J. H. Jones,[5] Cephise Cacho,[5] Richard T. Chapman,[5] and Russell S. Minns[1,a)]

AFFILIATIONS

[1]School of Chemistry, University of Southampton, Highfield, Southampton SO17 1BJ, United Kingdom
[2]Institute for Molecules and Materials, Radboud University, Heijendaalseweg 135, 6525 AJ Nijmegen, The Netherlands
[3]Center for Free-Electron Laser Science, Deutsches Elektronen-Synchrotron DESY, Notkestrasse 85, 22607 Hamburg, Germany
[4]The Hamburg Centre for Ultrafast Imaging, Universität Hamburg, Luruper Chaussee 149, 22761 Hamburg, Germany
[5]Central Laser Facility, STFC Rutherford Appleton Laboratory, Didcot, Oxfordshire OX11 0QX, United Kingdom

[a)]**Author to whom correspondence should be addressed:** r.s.minns@soton.ac.uk

ABSTRACT

The products formed following the photodissociation of UV (200 nm) excited CS_2 are monitored in a time resolved photoelectron spectroscopy experiment using femtosecond XUV (21.5 eV) photons. By spectrally resolving the electrons, we identify separate photoelectron bands related to the $CS_2 + h\nu \rightarrow S(^1D) + CS$ and $CS_2 + h\nu \rightarrow S(^3P) + CS$ dissociation channels, which show different appearance and rise times. The measurements show that there is no delay in the appearance of the S(^{1}D) product contrary to the results of Horio *et al.* [J. Chem. Phys. **147**, 013932 (2017)]. Analysis of the photoelectron yield associated with the atomic products allows us to obtain a S(^{3}P)/S(^{1}D) branching ratio and the rate constants associated with dissociation and intersystem crossing rather than the effective lifetime observed through the measurement of excited state populations alone.

I. INTRODUCTION

The dissociation dynamics of CS_2 have been the subject of numerous time and frequency resolved studies.[1–12,25,26] Despite its structural simplicity, it shows surprisingly complex dissociation dynamics involving competing dissociation channels and internal conversion (IC) and intersystem crossing (ISC) processes. Following excitation around 200 nm, the initial vibrational dynamics drive IC and ISC processes that lead to the formation of dissociation products. The dissociation leads to the formation of the electronic ground state of CS($^1\Sigma^+$) in conjunction with either the S(^{1}D) atomic fragment from the manifold of singlet excited states populated or the S(^{3}P) fragment following the ISC process. The overall reaction can therefore be represented as follows:

$$CS_2 + h\nu(200\ \text{nm}) \Longrightarrow \begin{matrix} CS(^1\Sigma^+) + S(^1D) \\ CS(^1\Sigma^+) + S(^3P). \end{matrix}$$

The excited state dynamics have been studied in detail with numerous ion yield and photoelectron spectroscopy experiments monitoring the dynamics in the initially excited singlet states.[1,3–5,8,12,25] Recent experiments utilizing XUV (21.5 eV) and VUV (9.3 eV) photons have extended these measurements to cover the time resolved detection of the formation of the dissociation products.[2,10] In the previous analysis of our XUV experiments, the populations of the singlet and triplet excited states and the formation of the dominant triplet state products were resolved and the lifetimes associated with the ISC and triplet dissociation were clearly identified.[2] The signals related to the singlet dissociation channel proved harder to isolate over the course of the full reaction, meaning the final yield and appearance time was difficult to confidently define. The analysis suggested an initial rapid rise in singlet population that was then slowed by the internal conversion process, which potentially stabilized the system against further singlet dissociation.[2]

In the VUV probe experiments of Horio *et al.*,[10] the formation of the $S(^1D)$ product was detected via ionization through the population of autoionizing resonances embedded in the $S^+(^4S_{3/2})$ ionization continuum. Direct ionization into the $S^+(^4S_{3/2})$ continuum is a spin forbidden process for the $S(^1D)$ product, but the population of autoionizing resonances means that this process can be driven indirectly. The rising signal associated with the formation of $S(^1D)$ products overlapped with the falling signal associated with the excited singlet state. The signal in the spectral region containing the $S(^1D)$ signal was therefore a mixture of the two components. In order to obtain a good fit to the signal, it was necessary to invoke a delay of some 400 fs after time zero for the rising signal associated with the appearance of $S(^1D)$ fragments. It was suggested that the delayed formation of the $S(^1D)$ product could be due to an indirect dissociation process where the outgoing wavepacket is trapped on a part of the excited state potential energy surface that has a lower ionization cross section.[10] The two experiments therefore provide quite contrasting pictures of the singlet dissociation process and the formation of the singlet product.

Another area where there remains some uncertainty is in the branching ratio (BR) of $S(^3P)/S(^1D)$. A number of measurements have been performed (predominantly at the slightly shorter wavelength of 193 nm) that provide widely varying values from 0.25 to 6.[9,11,13–19] The average value is around 3 but with a large variance.[9] It is very difficult to understand such a wide range of values apart from there perhaps being a strong wavelength dependence such that slight changes in vibrational state can cause large differences in BR.

Here, we perform a new analysis of the XUV (21.5 eV) photoelectron spectroscopy data and find a clear region of the photoelectron spectrum where we can monitor the formation of the $S(^1D)$ product and compare this with the previously measured $S(^3P)$ product. We also analyze the photoelectron yield associated with each product and obtain a new measure of the BR at an excitation wavelength of 200 nm.

II. EXPERIMENT

The experiment has previously been described by Smith *et al.*[2] such that we only provide brief details here. Approximately 1 μJ of 200 nm (6.2 eV) light is used as the pump, which is generated via sequential second harmonic generation and sum frequency generation processes in β-barium borate (BBO). The probe is generated via high harmonic generation using 500 μJ of 400 nm light, which is tightly focused into an argon filled gas cell. The seventh harmonic (57.7 nm, 21.5 eV) is isolated from the other harmonics produced in a time preserving monochromator. The isolated harmonic is subsequently reflection focused to the center of the interaction region where it overlaps the pump laser and molecular beam. The laser cross correlation time is 180 fs and is dominated by the duration of the 200 nm pulse. The CS_2 molecular beam is generated by the expansion of a 2% CS_2 in He mixture through a pulsed nozzle operating at 1 kHz (Amsterdam Cantilever).[20] The resulting beam is skimmed before entering the measurement chamber. The electrons resulting from the ionization of CS_2 are detected in a commercial electron time of flight spectrometer (Kaesdorf ETF11) with the laser polarizations of both the pump and probe parallel to the time of flight axis.

III. RESULTS AND DISCUSSION

In Fig. 1, we plot three photoelectron spectra associated with the ionization of ground state CS_2 and the dissociation products along with assignments based on the known ionization potentials.[21–23] In black, we plot the XUV photoelectron spectrum obtained from the ionization of the ground state of CS_2. The binding energy axis is defined as the ionizing photon energy (21.5 eV) minus the measured electron kinetic energy. The spectrum shows the positions of the X and A bands associated with the ionization of the ground state[23] and is used as the background for the experimental measurements. In the work of Smith *et al.*,[2] we subtracted the full intensity profile of this background signal from all delays. The background subtracted spectrum obtained in this way at asymptotically long time delays between pump and probe (i.e., after dissociation is complete) is plotted in blue in Fig. 1. The spectrum shows many of the peaks associated with the atomic and molecular products as well as depletion of the ground state signal. For the full analysis of the time dependent changes, this method of background subtraction provides a clear baseline from which changes can be measured but also masks signals related to product formation that may overlap with those associated with the ground state molecule. This effect can be most clearly seen in the region of the spectrum associated with the ionization into the CS_2 X-state, 10 eV, where the depletion is not uniform over the full peak profile. This is due to the overlap with a photoelectron energy associated with the ionization of the $S(^3P)$ fragment on the high binding energy edge.[21] A better approach in this situation is to subtract a scaled version of the background spectrum that matches the unpumped contribution to the overall signal, therefore only plotting the signal associated with molecules that are excited by the pump. In order to characterize the correct scaling, we look at the depletion of the X state signal from the ground state spectrum. As mentioned, at long delays, the asymptotic spectrum has signal associated with the ionization of the $S(^3P)$ product, which overlaps with the higher energy edge of the

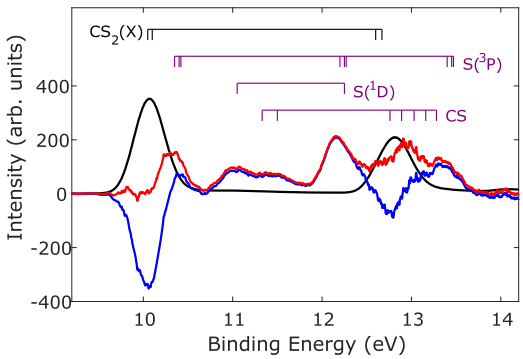

FIG. 1. Photoelectron spectrum obtained from ionization of the electronic ground state of CS_2 (black). The two peaks correspond to ionization into the ground and A states of the cation. Background subtracted photoelectron spectrum obtained after dissociation is complete, following the subtraction of the full background intensity (blue) and subtraction of a scaled version of the background equivalent to the unpumped ground state population (red). Combs above the spectra mark the expected positions of photoelectron bands based on the known ionization potentials.

X-state signal. The peak is sufficiently broad that the lower energy edge does not overlap the product signal such that we subtract a scaled version of the background that leaves the lower energy half of the X-state peak at an average of zero intensity following subtraction. This analysis suggests we are exciting 1.75% of all of the molecules that are subsequently ionized by the XUV probe. The results of the scaled subtraction on the asymptotic spectrum are plotted in red in Fig. 1. This background subtraction procedure for the removal of the unpumped background has the advantage that we can now see the full spectrum associated with the products formed and can start to quantify these.

In Fig. 2, we plot the full time resolved spectrum obtained following the subtraction of the unpumped background over the energy region that covers the product formation. The same scaled background subtraction is used at each time point. The spectrum shows the depletion of the ground state features and the transition to the spectrum associated with the products formed. In the previous analysis of these data, we could quantify the appearance of the triplet state product, which correlated well with the measured excited state dynamics. The singlet state formation was much less easily defined with the signal masked by the dominant triplet state products formed. Based on the spectrum plotted in Fig. 1, we see the clearest product state signal between the two main ground state features between 10.5 eV and 12.5 eV. The time dependent spectrum shows that the lower energy region associated with formation of the $S(^1D)$ product rises more rapidly than the $S(^3P)$ product.

In order to quantify this, in Fig. 3, we plot the integrated photoelectron yield between 10.8 eV–11.1 eV and 12.1 eV–12.2 eV, which correspond to the formation of the $S(^1D)$ and the $S(^3P)$ products, respectively. The $S(^1D)$ signal is seen to rise more rapidly than the $S(^3P)$ signal that, as shown in Ref. 2, rises after population and subsequent decay of the excited triplet electronic states of CS_2. To quantify this difference and to analyze the temporal profile of each product in a unified way, we use the same kinetic model as used by Smith *et al.*[2] The model breaks down the dynamics of the system into five distinct

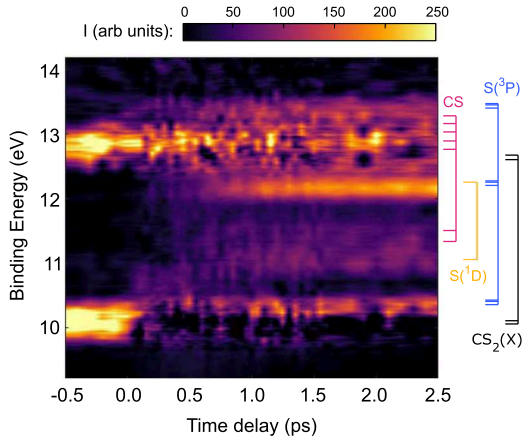

FIG. 2. Time resolved photoelectron spectrum following scaled background subtraction covering the energy region associated with the dissociation products formed. Assignments of the spectral features are given by the combs on the right-hand side of the figure.

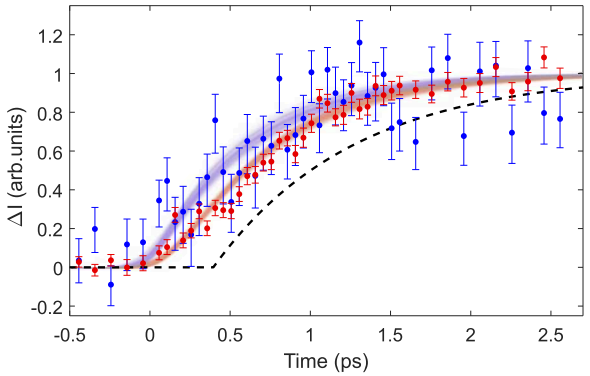

FIG. 3. Integrated photoelectron yield across the energy bands associated with the $S(^1D)$ (blue) and $S(^3P)$ (red) products. Error bars are obtained from a bootstrap analysis of the data, with the shaded areas representing the range of fits obtained in this analysis to Eqs. (1) and (2). The obtained appearance times for the singlet and triplet products are 518 ± 27 fs and 685 ± 14 fs, respectively. The black dashed line represents the expected signal based on the model and fit parameters for the singlet formation observed in the work of Horio *et al.*[10]

populations that track the dynamics of the system. Absorption of a photon transfers the population from the ground state, $CS_2(X)$, into the excited singlet states, $CS_2(S)$. The $CS_2(S)$ population decays into the excited triplet states, $CS_2(T)$, leading to the formation of triplet dissociation products, $S(^3P)$. The population that does not transfer into the triplet states dissociates to form the singlet, $S(^1D)$, dissociation product. The singlet and triplet dissociation pathways form parallel competing reactions given in the following reaction scheme:

$$\begin{array}{l} CS_2(X) \xrightarrow{h\nu} CS_2(S) \xrightarrow{k_{SD}} CS + S(^1D) \\ \qquad\qquad\quad \searrow^{k_{ISC}} \\ \qquad\qquad\quad CS_2(T) \xrightarrow{k_{TD}} CS + S(^3P) \end{array},$$

where k_{SD} and k_{ISC} are the rate constants associated with the decay of the initially excited singlet states into the singlet dissociation channel and into the excited triplet state, respectively. The ratio of k_{ISC} to k_{SD} then defines the branching between the two dissociation pathways, and the total decay rate of the excited singlet state is given by $K_S = k_{SD} + k_{ISC}$. The k_{TD} rate constant then defines the decay rate of the triplet state to dissociated products and $h\nu$ represents the laser pulse parameters that define the excitation step. By applying this model, we discretize the population into five distinct chemical species and obtain equations that define the time-dependent intensity of each chemical species and include the convolution with the instrument response function defined by the laser cross correlation. The equations used for the atomic products formed are then given by

$$I_{S(^1D)} = A_1\left(\left[1+\mathrm{erf}\left(\frac{t}{\sqrt{2}\sigma}\right)\right] - e^{-tK_S}e^{\frac{(\sigma K_S)^2}{2}}\left[1+\mathrm{erf}\left(\frac{t-\sigma^2K_S}{\sqrt{2}\sigma}\right)\right]\right), \quad (1)$$

$$I_{S(^3P)} = A_2\left(\frac{K_S - k_{TD}}{K_S k_{TD}}\left[1 + \mathrm{erf}\left(\frac{t}{\sqrt{2}\sigma}\right)\right] - e^{-tK_{TD}} e^{\frac{(\sigma K_{TD})^2}{2}} \times \left[1 + \mathrm{erf}\left(\frac{t - \sigma^2 K_{TD}}{\sqrt{2}\sigma}\right)\right] + e^{-tK_S} e^{\frac{(\sigma K_S)^2}{2}}\left[1 + \mathrm{erf}\left(\frac{t - \sigma^2 K_S}{\sqrt{2}\sigma}\right)\right]\right), \quad (2)$$

where A_x are amplitude terms that define the maximum yield, t is the pump–probe delay, σ defines the laser cross correlation width, and all other terms are as defined above. We note that although we only present the data associated with the products formed here, the fits performed use the full dataset including the populations of the bound molecular states, as presented by Smith *et al.*[2] In order to obtain errors on the fit parameters, we perform a bootstrap analysis of the full dataset, the results of which are plotted in Fig. 3. The red and blue shaded regions show the range of fits obtained from the bootstrap analysis, which all show clear differences between the singlet and triplet formation. The values obtained from the fits are consistent with the previous analysis across all populations considered, and a rise time constant for the S(^{1}D) product of 617 ± 37 fs is obtained. This is in line with the previously measured lifetime of the singlet excited state and consistent with a prompt dissociation of the CS_2 molecule. We see no evidence of a delayed appearance of the dissociation products, which instead show an increase in line with a kinetically controlled dissociation of the singlet state population. An alternative approach to quantify the appearance of the fragments is through the appearance time defined as the delay at which the intensity reaches 50% of the its maximum. The appearance times for the S(^{1}D) and S(^{3}P) are 517 ± 27 fs and 685 ± 14 fs, respectively. This is quite different to the work of Horio *et al.*[10] where a 393 fs induction time delay between initial excitation and the beginning of the rise of the S(^{1}D) signal was observed. They also observed a much slower rise time constant of 875 fs. To highlight the difference in appearance, we plot a dashed line in Fig. 3 showing the S(^{1}D) product signal based on the model and fit parameters of Horio *et al.*[10] but utilizing our laser cross correlation width as a dashed line in Fig. 3. The dashed line is a poor fit to the data, suggesting that any induction time is minimal. We have further tested this by fitting our data to the model of Horio *et al.* In all fits, the induction time converged to a value of close to 0. We suggest that the delayed appearance of the S(^{1}D) product in the VUV experiments of Horio *et al.*[10] may be due to the existence of a critical C–S separation for the resonant excitation and autoionization dynamics required for detection. Such an effect is often seen in the detection of dissociation products via resonance enhanced multiphoton ionization (REMPI) detection of products where critical distances can be very large. A careful analysis of the resonance conditions for REMPI detection of the I fragment from the photolysis of CH_3I puts this distance on the order of 13 Å.[24] If there is a similar situation in the VUV experiments, the delay would correspond to the time taken to reach this critical distance, and the long time constant associated with the subsequent rise would then reflect the very broad velocity distribution of the S(^{1}D) fragments. Given the much lower ultimate velocity of the S fragments in CS_2[6] compared with the CH_3I example, the 400 fs delay would correspond to a critical separation of around 4 Å.

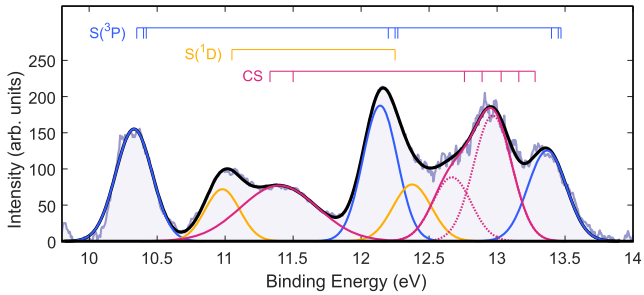

FIG. 4. Deconvolution of the scaled background subtracted photoelectron spectrum used to obtain the S(^{3}P)/S(^{1}D) branching ratio. The black line represents the total fit to the scaled background subtracted spectrum, which is plotted as a pale blue line. The individual Gaussian contributions to the overall fit are also plotted and color-coded to match the color of the combs.

Finally, we perform a deconvolution of the background-subtracted photoelectron spectrum based on a combination of Gaussians centered on the expected positions of the fragment photoelectron peaks, shown in Fig. 4. The deconvolution allows us to take the photoelectron yield for the S(^{1}D) and S(^{3}P) products as measured by the sum total of all of the peak areas associated with each atomic fragment. For the CS signal around 12.8 eV, we use a sum of two Gaussians to approximate the vibrational structure observed in previous high resolution experiments.[22] No further scaling is applied due to the ionization cross section at the probe wavelength being approximately equal for each S electronic state.[18] Performing this analysis, we obtain a S(^{3}P)/S(^{1}D) branching ratio of 2.3, which is in good agreement with the average value at 193 nm. We are unaware of any measurements at this exact pump wavelength. Based on the measured branching ratio and assuming that the branching is defined by the competition between singlet dissociation and ISC, we obtain time constants of 885 ± 50 fs and 2.0 ± 0.1 ps for the ISC and singlet dissociation processes, respectively.

IV. SUMMARY

We have presented a new analysis of experimental measurements that monitor the formation of dissociation products of CS_2 using a femtosecond XUV (21.5 eV) photoelectron spectroscopy probe. Through deconvolution of the photoelectron spectrum associated with all of the final products, we obtain a product BR, S(^{3}P)/S(^{1}D), of 2.3. By measuring both the branching ratio and effective rate constants associated with the excited state populations, we obtain the true time constants that define the branching between the dissociation pathways. The key parameters obtained from the

TABLE I. Summary of key parameters obtained from the data analysis. Time constants, τ_x, as defined in the text and obtained from the fit, branching ratio, BR, obtained from the deconvolution of the final spectrum, and appearance times, T_x, associated with the singlet and triplet state products.

τ_{SD} ($1/k_{SD}$)	τ_{ISC} ($1/k_{ISC}$)	τ_S ($1/K_{SD}$)	BR	T_S	T_T
2.0 ± 0.1 ps	885 ± 50 fs	617 ± 37 fs	2.3	518 ± 27 fs	685 ± 14 fs

analysis are summarized in Table I, which contains the obtained time constants, appearance times, and the branching ratio. The measurements allow us to monitor the real time formation of both atomic products and show no evidence of a delayed formation of the S(^{1}D) fragment, as previously observed when using a lower energy probe.[10]

ACKNOWLEDGMENTS

The authors thank the STFC for access to the Artemis facility. R.S.M. acknowledges the Leverhulme Trust (Grant No. RPG-2013-365) for research support and for studentship (A.D.S.) funding. R.S.M. thanks the Royal Society for funding (Grant Nos. UF100047, UF150655, and RG110310). E.M.W. thanks the University of Southampton for a studentship. D.A.H. was supported by the excellence cluster "The Hamburg Center for Ultrafast Imaging-Structure, Dynamics and Control of Matter at the Atomic Scale" of the Deutsche Forschungsgemeinschaft (Grant Agreement No. CUI, DFG-EXC1074), the European Research Council through the Consolidator Grant COMOTION (Award No. Küpper-614507), and the Helmholtz Gemeinschaft through the "Impuls-und Vernetzungsfond." We thank Phil Rice (Artemis) for technical assistance.

DATA AVAILABILITY

The data that support the findings of this study are available from the corresponding author upon reasonable request.

REFERENCES

[1]C. Z. Bisgaard, O. J. Clarkin, G. Wu, A. M. D. Lee, O. Gessner, C. C. Hayden, and A. Stolow, "Time-resolved molecular frame dynamics of fixed-in-space CS_2 molecules," Science **323**, 1464–1468 (2009).

[2]A. D. Smith, E. M. Warne, D. Bellshaw, D. A. Horke, M. Tudorovskya, E. Springate, A. J. H. Jones, C. Cacho, R. T. Chapman, A. Kirrander, and R. S. Minns, "Mapping the complete reaction path of a complex photochemical reaction," Phys. Rev. Lett. **120**, 183003 (2018).

[3]P. Farmanara, V. Stert, and W. Radloff, J. Chem. Phys. **111**, 5338 (1999).

[4]T. Horio, R. Spesyvtsev, and T. Suzuki, "Simultaneous generation of sub-20 fs deep and vacuum ultraviolet pulses in a single filamentation cell and application to time-resolved photoelectron imaging," Opt. Express **21**, 22423–22428 (2013).

[5]R. Spesyvtsev, T. Horio, Y.-I. Suzuki, and T. Suzuki, J. Chem. Phys. **142**, 074308 (2015).

[6]M. Brouard, E. K. Campbell, R. Cireasa, A. J. Johnsen, and W.-H. Yuen, "The ultraviolet photodissociation of CS_2: The S(^{1}D$_2$) channel," J. Chem. Phys. **136**, 044310 (2012).

[7]D. Bellshaw, R. S. Minns, and A. Kirrander, "Correspondence between electronic structure calculations and simulations: Nonadiabatic dynamics in CS_2," Phys. Chem. Chem. Phys. **21**, 14226–14237 (2019).

[8]D. Bellshaw, D. A. Horke, A. D. Smith, H. M. Watts, E. Jager, E. Springate, O. Alexander, C. Cacho, R. T. Chapman, A. Kirrander, and R. S. Minns, "*Ab initio* surface hopping and multiphoton ionisation study of the photodissociation dynamics of CS_2," Chem. Phys. Lett. **683**, 383–388 (2017), Ahmed Zewail (1946-2016) Commemoration Issue of Chemical Physics Letters.

[9]T. N. Kitsopoulos, C. R. Gebhardt, and T. P. Rakitzis, "Photodissociation study of CS_2 at 193 nm using slice imaging," J. Chem. Phys. **115**, 9727–9732 (2001).

[10]T. Horio, R. Spesyvtsev, Y. Furumido, and T. Suzuki, J. Chem. Phys. **147**, 013932 (2017).

[11]I. M. Waller and J. W. Hepburn, "Photofragment spectroscopy of CS_2 at 193 nm: Direct resolution of singlet and triplet channels," J. Chem. Phys. **87**, 3261–3268 (1987).

[12]P. Hockett, C. Z. Bisgaard, O. J. Clarkin, and A. Stolow, Nat. Phys. **7**, 612 (2011).

[13]W. B. Tzeng, H. M. Yin, W. Y. Leung, J. Y. Luo, S. Nourbakhsh, G. D. Flesch, and C. Y. Ng, "A 193 nm laser photofragmentation time-of-flight mass spectrometric study of CS_2 and CS_2 clusters," J. Chem. Phys. **88**, 1658–1669 (1988).

[14]W. S. McGivern, O. Sorkhabi, A. H. Rizvi, A. G. Suits, and S. W. North, J. Chem. Phys. **112**, 5301–5307 (2000).

[15]S. C. Yang, A. Freedman, M. Kawasaki, and R. Bersohn, "Energy distribution of the fragments produced by photodissociation of CS_2 at 193 nm," J. Chem. Phys. **72**, 4058–4062 (1980).

[16]M. C. Addison, R. J. Donovan, and C. Fotakis, "Resonance fluorescence study of electronically excited sulphur atoms: Reactions of S(3^1 D$_2$)," Chem. Phys. Lett. **74**, 58–62 (1980).

[17]V. R. McCrary, R. Lu, D. Zakheim, J. A. Russell, J. B. Halpern, and W. M. Jackson, "Coaxial measurement of the translational energy distribution of CS produced in the laser photolysis of CS_2 at 193 nm," J. Chem. Phys. **83**, 3481–3490 (1985).

[18]M. Barthel, R. Flesch, E. Rühl, and B. M. McLaughlin, Phys. Rev. A **91**, 013406 (2015).

[19]D. Xu, J. Huang, and W. M. Jackson, "Reinvestigation of CS_2 dissociation at 193 nm by means of product state-selective vacuum ultraviolet laser ionization and velocity imaging," J. Chem. Phys. **120**, 3051–3054 (2004).

[20]D. Irimia, D. Dobrikov, R. Kortekaas, H. Voet, D. A. van den Ende, W. A. Groen, and M. H. M. Janssen, Rev. Sci. Instrum. **80**, 113303 (2009).

[21]L. Zuin, F. Innocenti, M. L. Costa, A. A. Dias, A. Morris, A. C. S. Paiva, S. Stranges, J. B. West, and J. M. Dyke, "An initial investigation of S and SH with angle resolved photoelectron spectroscopy using synchrotron radiation," Chem. Phys. **298**, 213–222 (2004).

[22]N. Jonathan, A. Morris, M. Okuda, D. J. Smith, and K. J. Ross, "Photoelectron spectroscopy of transient species: The CS molecule," Chem. Phys. Lett. **13**, 334–336 (1972).

[23]D. W. Turner, *Molecular Photoelectron Spectroscopy*, 1st ed. (Wiley, 1970), ISBN: 047189320X.

[24]M. L. Murillo-Sánchez, J. González-Vázquez, M. E. Corrales, R. De Nalda, E. Martínez-Núñez, A. García-Vela, and L. Bañares, J. Chem. Phys. **152**, 014304 (2020).

[25]D. Townsend, H. Satzger, T. Ejdrup, A. M. D. Lee, H. Stapelfeldt, and A. Stolow, J. Chem. Phys. **125**, 234302 (2006).

[26]R. J. Hemley, D. G. Leopold, J. L. Roebber, and V. Vaida, J. Chem. Phys. **79**, 5219 (1983).